J Solid State Electrochem (2001) 5: 74–79

SHORT COMMUNICATION

W.-F. Zhang · P. Schmidt-Zhang · G. Kossmehl

Study of the electrosynthesis of poly(3-butylthiophene) and its semiconductor properties

Received: 29 July 1999 / Accepted: 15 November 1999

Abstract The mechanism of the electrosynthesis of poly(3-butylthiophene) (PBuT) was studied by cyclic voltammetry and potential step methods in comparison with polybithienyl. The anodic oxidation polymerization of the 3-butylthiophene underwent two steps: oligomer formation and further polymerization to form the polymer. The doping level of the PBuT increases with the cycle number of the potential sweeps during polymerization. The current responses to the potential steps indicate a nucleation and nuclei growth process which is repeated layer to layer. The differential capacity (C_d) and photocurrent were measured at the PBuT films in the aqueous electrolyte solution. The C_d^{-2} vs. E plot shows two regions of linearity, one with a negative slope and the other with a positive slope in different potential regions, which give the same flat-band potential. This indicates that the PBuT film exhibits both p-type and n-type features of a semiconductor at differrent potential regions. The cathodic photocurrent spectrum was analysed by the $(j_{ph}hv)^{2/n}$ vs. hv plots, giving band gap energies of 2.41 eV for $n = 1$ and and 2.01 eV for $n = 4$.

Key words Electrosynthesis · Poly(3-butylthiophene) · Differential capacity · Photocurrent · Semiconductor

Introduction

Research on polythiophene (PT) and its derivatives has rapidly developed owing to their good electrochemical and electrical properties. Especially, the 3-alkylthiophenes have attracted increasing interest [1–4]. To the present, poly(3-alkylthiophenes) (PATs) with alkyl chains containing 1–20 carbons have been reported. However, most reports are about studies of poly(3-methylthiophene) [5–8]. Poly(3-butylthiophene) (PBuT) has been reported in several papers [9–11], but the photocurrent and differential capacity of PBuT films were rarely mentioned [12]. Quantitative analysis of the PBuT electrosynthesis process is difficult owing to its solubility in common organic solvents. Nevertheless, PBuT films have higher electric conductivity and better electrochemical stability in organic electrolyte solutions than polybithienyl (PBT) films [13]. This is interesting for the application of electrically conducting organic polymers. Therefore, we have systematically studied the electrosynthesis process of PBuT and obtained the optimal conditions for the formation of PBuT films having compact structure and fine morphology. In the present paper we report the results of a study in comparison with the electrosynthesis mechanism for PBT films reported in our previous paper [14]. The differential capacity and photocurrent at the PBuT film was measured and analysed by means of the theory of the semiconductor|solution interface.

W.-F. Zhang (✉) · G. Kossmehl
Institute for Organic Chemistry,
Free University of Berlin, Takustrasse 3,
14195 Berlin, Germany

P. Schmidt-Zhang
Kurt-Schwabe-Institut für Mess- und
Sensortechnik e.V. Meinsberg, Fabrikstrasse 69,
04720 Ziegra-Knobelsdorf, Germany

Experimental

A potentio/galvanostat (EG & G) and a three-electrodes titration cell (Metrohm) were used for the PBuT electrosynthesis and electrochemical measurements. The working electrode (WE) was a Pt rotating disc (0.071 cm^2). A twisted Pt wire served as the counter electrode (CE) and the reference electrodes were Ag/AgCl for organic solutions and a SCE for aqueous solutions, respectively. A two-phase lock-in amplifier (278 EG & G) was used for the capacity measurements. Photocurrent measurements were carried out in a three-electrode photoelectrochemical cell with a quartz window. A xenon lamp with a power of 150 W served as the light source connected to a monochromator with wavelengths from 250 nm to 1500 nm and a light chopper working at a frequency of 0.1 Hz. The results were recorded by a *x*-*y*-*t* recorder (Linseis).

Commercial 3-butylthiophene (BuT) (99.2%) and acetonitrile (MeCN) (HPLC grade) were used as monomer and solvent for the

electrosynthesis, respectively. $LiClO_4$ was the supporting electrolyte for all experimental solutions. The experimental solutions were deoxygenated by argon (99.999%).

Results and discussion

Study of the electrosynthesis of PBuT film

It is difficult to deposit PBuT film upon the surface of a metal electrode because of its solubility in common solvents such as $CHCl_3$, CH_2Cl_2 and THF. An attempt to electrosynthesize PBuT on a Pt electrode in a propylene carbonate electrolyte solution at room temperature failed, which was not investigated further. However, it has been reported that, at 5 °C, PBuT film can be electrochemically prepared in propylene carbonate electrolyte [10]. Under a N_2 (99.999%) atmosphere we have obtained only soluble oligomers instead of PBuT at a Pt electrode in MeCN + 0.1 M $LiClO_4$ + 0.05 M BuT. The corresponding cyclic voltammograms (CVs) show only anodic currents without any cathodic current, because the soluble oligomers diffused to the CE surface where they were reduced. It is notable that PBT electrosynthesis was very successful under a N_2 atmosphere [13, 14]. Under an Ar (99.999%) atmosphere the PBuT electrosynthesis was successful. The conditions for galvanostatic synthesis of PBuT films are more critical than that of the CV method. In order to obtain a compact PBuT film with a fine morphology, the applied current density has to be higher than 10 mA cm^{-2}. When the current density is smaller than 1 mA cm^{-1}, almost no PBuT was deposited on the WE surface in spite of the high BuT monomer concentration of 0.5 M.

In order to study the mechanism of the BuT anodic polymerization, the CV at a rotating Pt disc electrode (1000 rpm) and potential step experiments at a stationary Pt electrode were performed in MeCN + 0.1 M $LiClO_4$ + BuT with variable concentrations, deoxygenated by Ar. The cyclic votammograms (CVGs) are shown in Fig. 1. The oxidation potential E^{ox}_{BuT} of BuT monomer in MeCN was determined as being 1.25 V. In the first cycle the anodic current initially increases ($E < 1.5$ V) very slowly, then it rises rapidly and linearly until the potential sweep reverse. In the backward sweep this current drops, but it is higher than that in the forward sweep at the same electrode potential (Fig. 1a). This means that the current-potential polarization curve (j vs. E) is in the Tafel region instead of the diffusion region. Assuming this electrode process is a single reaction, then the Tafel equation can be used to analyse the current behaviour in order to obtain kinetic information [15, 16]. The E vs. log j plot of the first anodic forward sweep shows two linearities with different slopes: $(ba)_1$ at $E = 1.3$–1.5 V and $(ba)_2$ at 1.6–1.8 V, where $(ba)_1 > (ba)_2$. This indicates that the polymerization by anodic oxidation of the BuT monomer underwent two steps: oligomer formation and then polymerization to form the polymer, i.e.

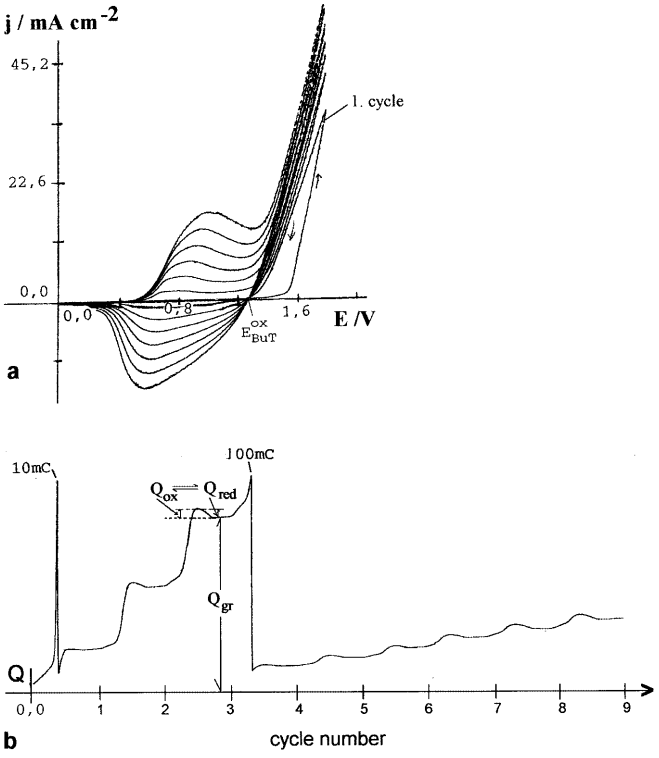

Fig. 1a Cyclic voltammogram and **b** change of the charges during the potential sweep at a Pt rotating disc electrode (1000 rpm) in MeCN + 0.1 M $LiClO_4$ + 0.1 M BuT; $v = 50$ mV s^{-1}

$$\text{Monomer} \xrightarrow{\text{step 1}} \text{Oligomer} \xrightarrow{\text{step 2}} \text{Polymer} \qquad (1)$$

The oligomer has a lower oxidation potential and is more easily oxidized than the BuT monomer. The currents of the monomer oxidation and oligomer oxidation overlap each other, so that the anodic current in the backward sweep is higher than the one in the forward sweep at the same potential in the first cycle, as mentioned above.

The first cycle of the cyclic voltammogram (CVG) shows a cathodic current peak which is repeated in the second cycle and is coupled with an anodic current peak at a potential lower than the oxidation potential E^{ox}_{BuT} of the BuT monomer. This pair of current peaks corresponds to the reduction and oxidation of the PBuT, which has a lower oxidation potential than the BuT monomer. They cannot be removed by electrode rotation or by high monomer concentration. This indicates that the pair of current peaks can be caused only by diffusion of the dopant ClO_4^- anions in the solid state PBuT film during its reduction and oxidation process in the cyclic potential sweeps, which is similar to that in PBT electrosynthesis [14].

The redox charges of the PBuT film, $Q_{ox} = Q_{red}$, and the chain growth charge Q_{gr} (defined in Fig. 1b) are proportional to the cycle number of the potential sweeps, respectively (Fig. 2a, b). However, the ratio of Q_{ox}/Q_{gr} defined as the doping level of the PBuT film according to the R-R mechanism of thiophene poly-

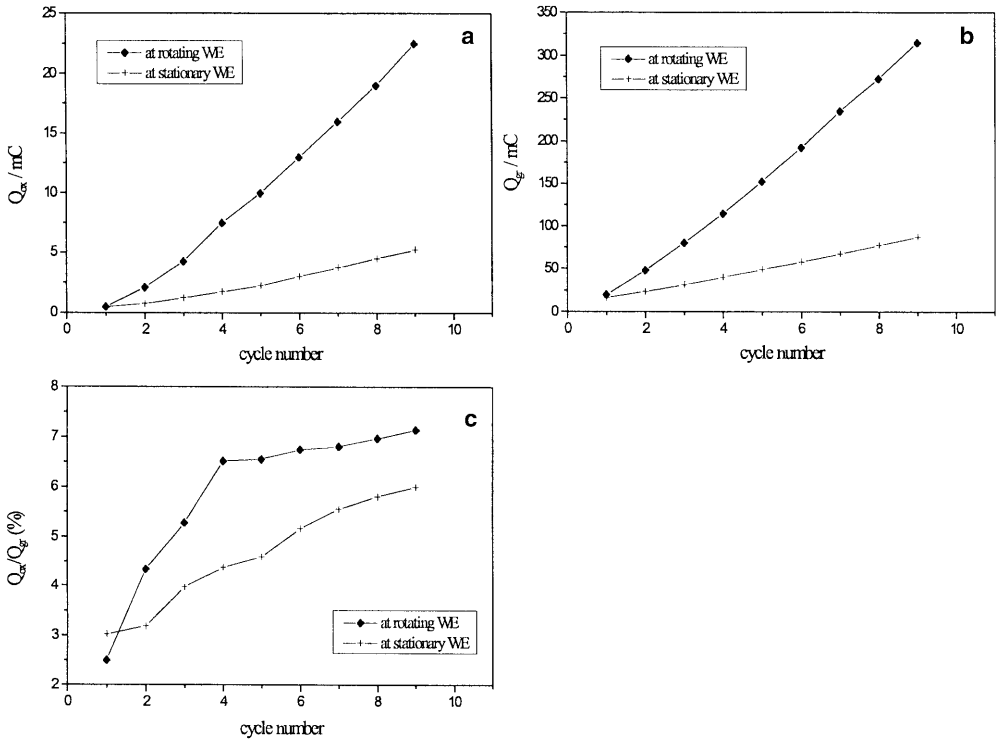

Fig. 2 Changes **a** of the PBuT oxidation charge Q_{ox}, **b** of the chain growth charge Q_{gr}, **c** of the ratio of Q_{ox}/Q_{gr} with the cycle number of the potential sweeps for PBuT electrosynthesis by CV ($v = 50$ mV s^{-1}) at a Pt rotating disc electrode (1000 rpm) and a Pt stationary electrode, respectively, in MeCN + 0.1 M $LiClO_4$ + 0.1 M BuT

merization [14, 17], increases with the cycle number (Fig. 2c). This is different from that of PBT films, where the doping level of PBT is kept constant during the overall polymerization process [13, 14]. The PBuT films formed at the rotating disc electrode have higher doping levels than those formed at the stationary electrode (Fig. 2c). The doping levels of the PBuT films are generally lower than those of PBT films. Nevertheless, PBuT film has a better electrical conductivity than PBT film formed under the same conditions [13]. This can be attributed to the butyl group at the β-position of the thiophene ring, which has a steric effect on the conjugated π-system and on the chain structure, leading to an increase in electron mobility in the PBuT film [18, 19].

Several potential steps from 0 V up to 1.2 V, 1.4 V, 1.6 V and 1.8 V, respectively, were carried out at a stationary Pt electrode in MeCN + 0.1 M $LiClO_4$ + 0.5 M BuT solution. The current response curves are shown in Fig. 3. The current response for the potential step of 1.2 V, lower than the oxidation potential of BuT (E^{ox}_{BuT}), is almost zero and no PBuT film was obtained (curve 1 in Fig. 3). The anodic currents for 1.4 V and 1.6 V (curves 2 and 3 in Fig. 3) at first drop with time rapidly to a minimum, then rise with time, following the power law:

$$j \propto (t - t_0)^x \qquad (2)$$

and finally they increase slowly (where t_0 is the time at the current minimum; $x = 0.31$ for the potential step of 1.4 V). This current behaviour indicates a nucleation and nuclei growth process by a layer-to-layer mechanism similar to PBT formation [14]. This process is concluded from the micrographs of the PBuT films (Fig. 4). The current at 1.8 V (curve 4 in Fig. 3) increases directly with time. This indicates that the anodic BuT polymerization was kinetically controlled, which is in agreement with the behaviour of the anodic currents of the CVG in Fig. 1a and is different from the case of the PBT electrosynthesis where the current of the high potential step dropped with time, following the Cottrell equation [14].

The PBuT film can be reversibly reduced and oxidized. Figure 4 shows an oxidized PBuT film (a) and a reduced PBuT film (b). The former is green with inserts of a yellow-red colour and the latter has a yellow-red colour with green points, which implies that the redox reactions of PBuT were not completely carried out, i.e. PBuT films are a mixture of the polymer cations and neutral polymer molecules. The PBuT cations are dominant in the oxidized form and a minor component

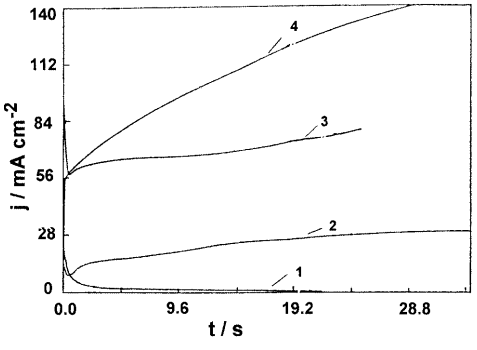

Fig. 3 Current–time response curves to the potential steps from 0 V to: *1* 1.2 V, *2* 1.4 V *3* 1.6 V, *4* 1.8 V at Pt in MeCN + 0.1 M $LiClO_4$ + 0.5 M BuT

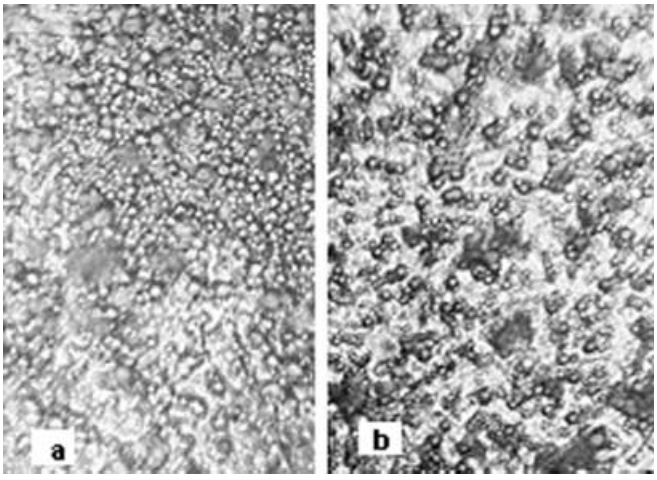

Fig. 4a,b Micrographs of the PBuT films: **a** in oxidized form, **b** in reduced form (enlargement: 930)

in the reduced form. This is different from the case of PBT, where the oxidized PBT film is blue and the reduced PBT film is red [13, 14].

Semiconductor properties of the PBuT films

From experience, the PBuT films formed by the CV method have a more compact structure and a finer morphology than that obtained by the galvanostatic method. Therefore, all PBuT films used for the differential capacity and photocurrent measurements were prepared by the CV method. The semiconductor properties of PBuT were proved by the results of the differential capacity C_d and photocurrent j_{ph}. The C_d vs. E curve and corresponding C_d^{-2} vs. E plot for a PBuT film with a thickness of 10 μm are shown in Fig. 5. The differential capacity has a similar order of magnitude to the space charge capacity of the inorganic semiconductor in the electrolyte solution [20]. The C_d^{-2} vs. E curve shows two regions of linearity with a negative slope and a positive slope, respectively, in different potential ranges. According to the Mott-Schottky equation

$$\frac{1}{C_d^2} = \frac{2}{\varepsilon\varepsilon_0 eN}|E - E_{fb}| - \frac{kT}{e} \tag{3}$$

where ε, ε_0, e, N, E_{fb}, k and T are semiconductor dielectric constant, vacuum dielectric constant, elementary charge, doping level of the semiconductor, flat band potantial, Boltzmann constant and absolute temperature, respectively; the negative slope represents a p-type semiconductor and the positive slope is valid for an n-type semiconductor. This implies that this PBuT film exhibits both p-type (at −0.4 to −0.1 V) and n-type (at

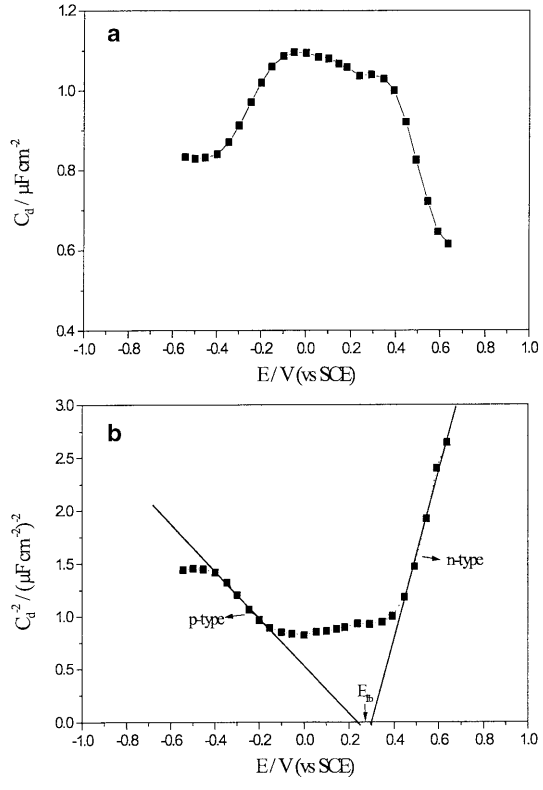

Fig. 5 Potential dependence of the differential capacity at a PBuT film (thickness 10 μm, doping level 1.2%) in H_2O + 0.2 M $LiClO_4$; modulation frequency 1 kHz. **b** C_d^{-2} vs. E plot corresponding to **a**

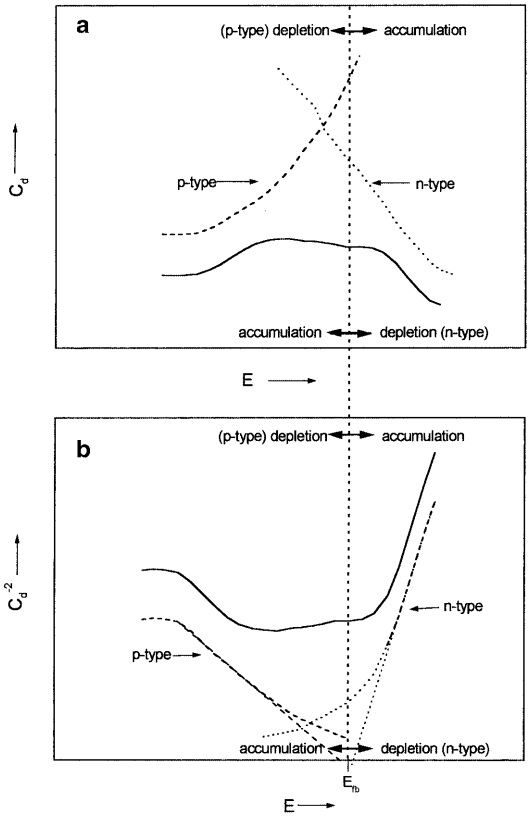

Fig. 6 Analysis **a** of the differential capacity and **b** of the C_d^{-2} vs. E plot in Fig. 5, where the *solid curves* are taken from Fig. 5 and the *dotted curves* are analyses of these curves

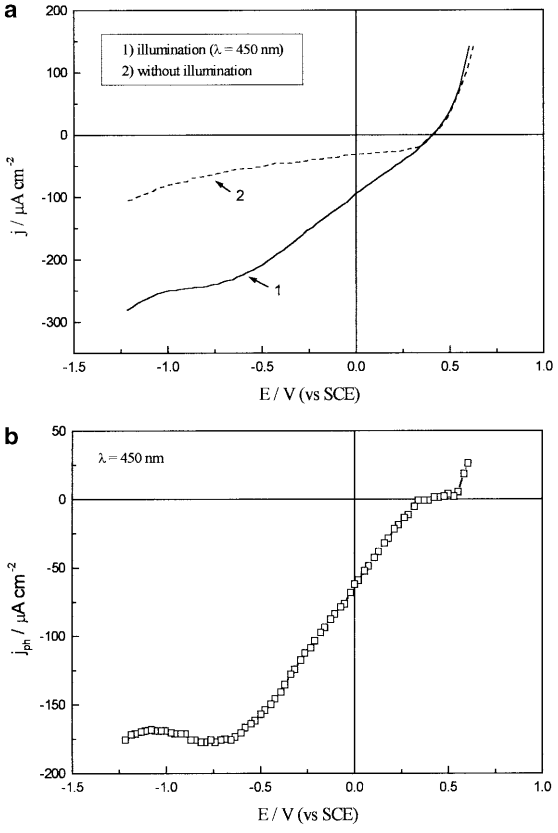

Fig. 7a,b *j* vs. *E* curves at a PBuT film in H_2O + 0.2 M $LiClO_4$: *1* illuminated by monochromatic light, $\lambda = 450$ nm, *2* without illumination; **b** photocurrent obtained from **a**

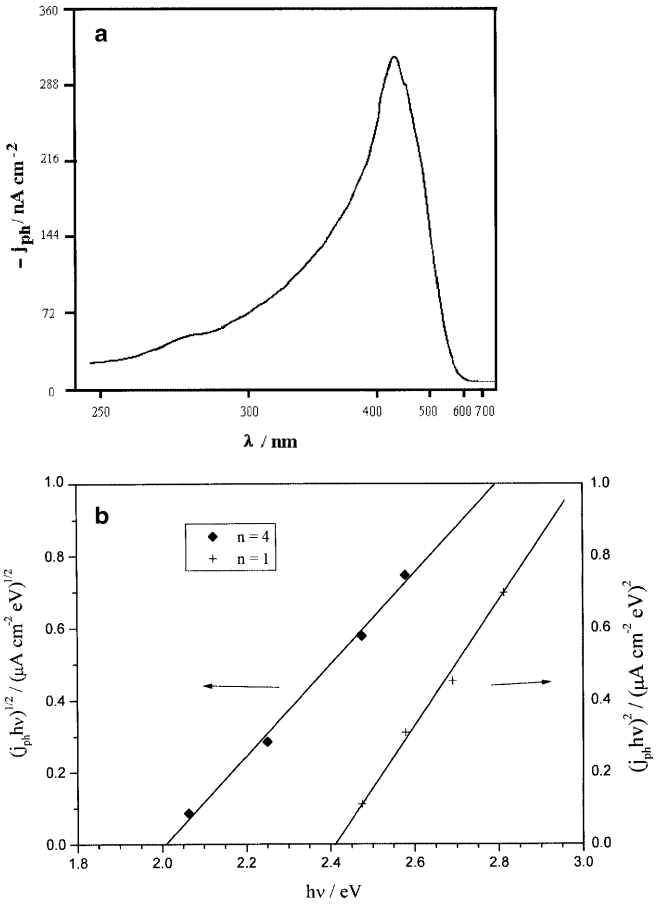

Fig. 8 **a** Cathodic photocurrent spectrum of a PBuT film in H_2O + 0.2 M $LiClO_4$ at 0.0 V; **b** $(j_{ph}h\nu)^{1/2}$ vs. $h\nu$ and $(j_{ph}h\nu)^2$ vs. $h\nu$ plots, taken from **a**

0.4–0.6 V) features of a semiconductor. The intercept points of both linearities of the C_d^{-2} vs. E plot at the E axis give the same flat-band potential, $E_{fb} = 0.27$ V for 25 °C (Fig. 5b). The C_d and C_d^{-2} curves may be considered as an overlapping of two single partial curves of the p-type and n-type, as shown in Fig. 6a and b. In the neighbourhood of the flat-band potential the accumulation state of the n-type is overlapped by the depletion state of the p-type ($E < E_{fb}$), whereas the accumulation state of the p-type is overlapped by the depletion layer of the n-type ($E > E_{fb}$), leading to a transition from p-type to n-type semiconductor like an n-p junction of a classical semiconductor.

A xenon lamp was used to illuminate the PBuT film during the electrode polarization. The current obtained under the illumination is obviously higher than the dark current (Fig. 7a). The difference between the illumination current and the dark current represents the photocurrent due to a photoeffect of the PBuT film under illumination (Fig. 7b), where the cathodic photocurrent shows a limit in the potential range of −1.0 V to −0.6 V, similar to that of PBT films [12, 13] and to the photocurrent of hydrogen evolution at a GaAs p-type semiconductor [21]. A small anodic photocurrent is clearly seen. This means that the PBuT film in this potential range behaved as an n-type semiconductor.

Figure 8a gives a cathodic photocurrent spectrum, obtained at a PBuT film which was preserved in the air for three months before measurement of the photocurrent. The photocurrent spectrum was analysed by using the Gaertner-Butler model [22, 23] on the basis of the theory of the semiconductor|solution interface suggested by Gerischer [20, 21]. The $(j_{ph}h\nu)^{2/n}$ vs. $h\nu$ plots, taken from the photocurrent spectrum, show two linearities at $\lambda = 440$–500 nm for $n = 1$ and at $\lambda = 480$–600 nm for $n = 4$, respectively (Fig. 8b). This photocurrent behaviour of the PBuT films is similar to that of PBT films [24]. According to the equation

$$(j_{ph}h\nu)^{2/n} = (e\Phi_0 WA_n)^{2/n}(h\nu - E_g) \quad (4)$$

the intercept points of the linearities at the $h\nu$ axis give the band gap energies of 2.41 eV for $n = 1$ and 2.01 eV $n = 4$ (Fig. 8b), where h, ν, Φ_o, W and E_g are respectively Planck's constant, frequency, total photon flux, thickness of the depletion layer and band gap energy of the semiconductor; A_n is a constant essentially representing the electronic transition probability and is independent of the illumination. The numbers $n = 1$ and $n = 4$ represent a direct transition and an indirect transition, respectively.

Conclusion

The conditions of PBuT electrosynthesis are critical. A good PBuT film should be prepared by the CV method in MeCN electrolyte solution. The doping level of the PBuT film can be controlled by the cycle number of the potential sweeps, because the doping level increases with the cycles. The differential capacity and photocurrent indicate that the PBuT film has both p-type and n-type features of a semiconductor in different potential regions, like the p-n transition in a classical semiconductor which is applied in solar cells or in rectifiers.

Acknowledgements The authors are greatly indebted to Professor W. Plieth (Institut fuer Physikalische Chemie und Elektrochemie, TU Dresden) for the opportunity to work in his laboratory.

References

1. El-Rashiedy OA, Holdcroft S (1996) J Phys Chem 100: 5481
2. Lapkowski M, Zagorska M, Bazer IK, Koziel K, Adampron (1991) J Electroanal Chem 310: 57
3. Chao F, Costa M, Jin G, Tian C (1994) Electrochim Acta 39: 197
4. Roncali J, Garreau R, Yassar A, Marque P, Garnier F, Lemaire M (1987) J Phys Chem 91: 6706
5. Marque P, Roncali J, Garnier F (1987) J Electroanal Chem 218: 107
6. Welzel HP, Kossmehl G, Stein HJ, Schneider J, Plieth W (1995) Electrochim Acta 40: 577
7. Micaroni L, Dini D, Decker F, De Paoli MA (1999) J Solid State Electrochem 3: 352
8. Nogueira AF, Micaroni L, Gazotti WA, De Paoli MA (1999) Electrochem Commun 1: 262
9. Elsenbaumer RC, Kwan Y, Miller GG, Eckhard H, Shacklette LW, Jow R (1987) Electron Prop Conjugated Polym. In: Springer Series in solid-state science, vol 76. Springer, Berlin Heidelberg New York, p 400
10. Kaeriyama K, Sato M, Tanaka S (1987) Synth Met 18: 233
11. Kulszewiez-Bajer I, Pawlicka A, Plenkiewicz J, Pron A (1989) Synth Met 30: 355
12. Zhang WF, Schmidt-Zhang P, Kossmehl G, Plieth W (1999) J Solid State Electrochem 3: 135
13. Zhang WF (1994) Thesis. Free University Berlin, Germany
14. Zhang WF, Plieth W, Kossmehl G (1997) Electrochim Acta 42: 1653
15. Vetter KJ (1961) Elektrochemische Kinetik. Springer, Berlin Heidelberg New York, pp 110, 218, 414
16. Bard AJ, Faulkner LR (1980) Electrochemical methods fundamental and applications. Wiley, New York, pp 103, 280
17. Waltman RJ, Bargon J (1986) Can J Chem 64: 76
18. Waltman RJ, Bargon J, Diaz AF (1983) J Phys Chem 87: 1459
19. Tourillon G, Garnier (1984) J Electroanan Chem 161: 51
20. Gerischer H (1990) Electrochim Acta 35: 1677
21. Gerischer H (1970) Semiconductor electrochemistry. In: Eyring H, Henderson D, Jost W (eds) Physical chemistry, an advanced treatise, vol IXA. Academic Press, New York, p 463
22. Gaertner W (1959) Phys Rev 116: 84
23. Butler MA (1977) J Appl Phys 48: 1914
24. Zhang WF, Schmidt-Zhang P, Kossmehl G (2000) J Solid State Electrochem 4: 225